

Ionization of Bases in Water: Structure and Stability of the $\text{NH}_4^+\cdots\text{OH}^-$ Ionic Forms in Ammonia–Water Clusters

Chengteh Lee and George Fitzgerald

Cray Research Inc., Eagan, Minnesota

Marc Planas and Juan J. Novoa*

Departamento de Química Física, Facultad de Química, Universidad de Barcelona, Av. Diagonal 647, 08028 Barcelona, Spain

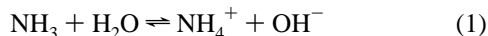
Received: November 15, 1995; In Final Form: February 7, 1996[⊗]

The structure and stability of the $\text{NH}_4^+\cdots\text{OH}^-$ ionic forms resultant from the equilibrium $\text{NH}_3 + \text{H}_2\text{O} \rightleftharpoons \text{NH}_4^+ + \text{OH}^-$ is analyzed by Hartree–Fock, second-order Moller–Plesset, and the Becke–Lee–Yang–Parr density functional. Our results show that a double ionic cluster $\text{NH}_4^+\cdots(\text{H}_2\text{O})_3\cdots\text{OH}^-$, in which three molecules are located between the NH_4^+ and OH^- ions, is stable and lies 5–10 kcal/mol higher than various neutral clusters containing one ammonia and four water molecules. The process of formation of the double ionic cluster from a geometrically similar neutral cluster is shown to be synchronic, with the two protons being simultaneously transferred. The MP2 and BLYP methods give a similar description of the structure and stability of these clusters.

Introduction

It is a well-known experimental fact that when a molecule of a compound B more basic than water is dissolved in an aqueous solution, one water molecule donates one of its protons to B and the ions BH^+ and OH^- are formed. A prototypical system for the study of this type of reaction can be the solutions of ammonia in water, a case in which $\text{B} = \text{NH}_3$. However, a detailed study of the proton-transfer process at the molecular level using ab initio methods has not been possible due to the lack of a reasonably small stable cluster of the double ionic $\text{BH}^+\cdots\text{OH}^-\cdots(\text{H}_2\text{O})_n$ system. In this work we will describe the structure of a small double ionic $\text{BH}^+\cdots\text{OH}^-\cdots(\text{H}_2\text{O})_n$ cluster with $n = 3$ which is a minimum in the potential energy surface of the whole system. We will discuss its stability against similar neutral clusters, analyzing the dynamics of such a transformation and the reason for the stability of the double ionic cluster. We should consider this cluster as a first step toward the study of the proton-transfer process in ammonia–water mixtures, as larger clusters are probably needed to describe such potentially important effects in this process as the solvent reorganization.

The presence of NH_4^+ and OH^- ions in water solutions is a well-established fact¹ and satisfies the following reaction:



The experimental equilibrium constant for this reaction² at room temperature is 1.77×10^{-5} , i.e., bigger than the autoionization constant for pure water. Therefore, the concentration of NH_4^+ and OH^- in water solutions, although small, 4.21×10^{-3} mol/dm³, is 4 orders of magnitude larger than the concentration of OH^- in pure water, and the ΔG value for the same reaction is 6.48 kcal/mol.

The ionic dissociation 1, however, is not detected in the gas phase or in some crystals with mixtures of ammonia and water. The absence of ionic forms in the first case can be explained due to the instability of the NH_4^+ and OH^- ions in the gas

phase: they are known³ to lie 185.8 kcal/mol above the energy of the neutral reactants and the equilibrium 1 is in this case strongly displaced to reactants. In the solid state, the ammonia and water mixtures can form hydrates. Among those possible the only two experimentally known up to now are the solid hydrates $\text{NH}_3 \cdot \text{H}_2\text{O}$ and $\text{NH}_3 \cdot 2\text{H}_2\text{O}$. The presence of NH_4^+ and OH^- in these crystals has been postulated,^{1,4} but their infrared spectra⁴ does not show any of the characteristic frequencies of the NH_4^+ and OH^- ions and instead resemble a superposition of the spectra of neutral NH_3 and H_2O , a fact that has been associated to a negligibly small concentration of the NH_4^+ and OH^- ions in these two crystals.

The previous experimental facts seem to indicate that the solvent plays an important role in reaction 1 stabilizing the formation of the ionic products in a way not possible in the gas phase and the solid hydrates $\text{NH}_3 \cdot \text{H}_2\text{O}$ and $\text{NH}_3 \cdot 2\text{H}_2\text{O}$. To understand the role played by the solvent and the differences between the solid and liquid phases indicated above, one need to have information at the molecular level on the structure of the ionized solution, i.e., the structure and stability of the hydrated $\text{NH}_4^+\cdots\text{OH}^-$ contraions in water solution, hereafter called $(\text{NH}_4^+\cdots\text{OH}^-)_{\text{aq}}$. Up to our knowledge, there is no detailed experimental or theoretical information on the structure of $(\text{NH}_4^+\cdots\text{OH}^-)_{\text{aq}}$, although the structure of each hydrated $(\text{NH}_4^+)_{\text{aq}}$ and $(\text{OH}^-)_{\text{aq}}$ ions is known both experimentally⁵ and theoretically.⁶

To obtain the information of interest here, one can resort to compute the structure of the $(\text{NH}_4^+\cdots\text{OH}^-)_{\text{aq}}$ system in small clusters of water, as a first step to understand the microscopic details of this complex in the bulk and on the ionic dissociation process (eq 1). In doing so, we will follow an approach similar to that already employed in our recent study of the autoionization of water, where the process was simulated using $\text{H}_3\text{O}^+ - (\text{H}_2\text{O})_3 - \text{OH}^-$ clusters,⁷ or in our study of the ionization of acids in water.⁸ These two studies showed that by inserting an adequate number of water molecules between the dissociated ions, one can have stable cluster structures which show the presence of the oppositely charged contraions. Using similar cluster structures, in this work we are going to test if one can

[⊗] Abstract published in *Advance ACS Abstracts*, April 1, 1996.

also find stable cluster structures which show the presence of the oppositely charged contraions, in this case, the $\text{NH}_4^+\cdots\text{OH}^-$ contraions. We will carry out the test with clusters of four water molecules in which three of the water molecules lie in between the NH_4^+ and OH^- ions and the fourth is that undergoing dissociation. As will be shown later, it is possible to find some stable cluster geometries showing the presence of the NH_4^+ and OH^- contraions. The geometrical structure of these clusters will be analyzed to understand its properties and stability, an important step toward a better understanding of these type of structures in the bulk.

Computational Details

The cluster geometries considered here were fully optimized at the Hartree-Fock (HF) and second order Moller-Plesset (MP2) levels using the 6-31+G(d,p) basis set and the GAUSSIAN-92 program.⁹ We also carried out density functional computations using the gradient corrected exchange-correlation energy functional of Becke¹⁰ and Lee-Yang-Parr¹¹ (BLYP), as implemented in the DGauss program.¹² It has been shown that the gradient-corrected density functionals are capable of reproducing the known properties of hydrogen-bonded complexes.¹³⁻¹⁸ In particular, the BLYP has been shown to give results in good agreement with these from MP2 computations for the structure and energetic properties of water clusters¹⁷ and also gave results similar to the MP2 method in the two studies we carried out on the ionization process of water and acids.^{7,8} The basis set employed in the BLYP computations was the recently developed triple- ζ basis set with polarization functions (TZ94P), whose exponents were optimized to produce the lowest atomic energy at the local density level.¹⁹

On the fully optimized geometries we performed a vibrational analysis at the HF, MP2, and BLYP levels in order to check the true nature of the minimum energy structures obtained in the optimization process. The zero-point energy was also computed using the data from the harmonic frequencies, and its influence on the binding energy of the clusters also taken into account. These corrections are just estimated upper limits of the true zero-point corrections due to the expected anharmonicity of some intermolecular vibrational modes.

Results and Discussion

We started our study by searching for the presence of possible minimum energy structures for the double ionic $\text{NH}_4^+(\text{H}_2\text{O})_n\text{OH}^-$ cluster. Any of these minimum-energy structures are isomer conformations of the cluster that are stable against local geometrical distortions, i.e., they are local minima on the potential energy surface of the complex. On these double ionic clusters, we will study its geometrical and electronic structure, its stability against the most likely neutral clusters of the same molecular composition, one ammonia and four waters and, finally, its stability against fragmentation into its constituent neutral or ionic fragments.

The minima located on a given potential energy surface depends of the selected starting geometry. In our case, to speed up our search, we used as starting point for the $\text{NH}_4^+(\text{H}_2\text{O})_n\text{OH}^-$ cluster the minimum energy geometry previously found for the $\text{H}_3\text{O}^+(\text{H}_2\text{O})_3\text{OH}^-$ cluster⁷ (see Figure 1a) and the H_3O^+ ion is substituted by the NH_4^+ ion, keeping three of the hydrogens of the NH_4^+ ion in the same spatial positions held by the hydrogens of the H_3O^+ ion, while the fourth hydrogen is pointing outward (see Figure 1b). This seems a reasonable choice because the H_3O^+ and NH_4^+ ions have a similar spatial arrangement of their hydrogens and both have a similar strength in the acidity scale, one can expect that both clusters could have

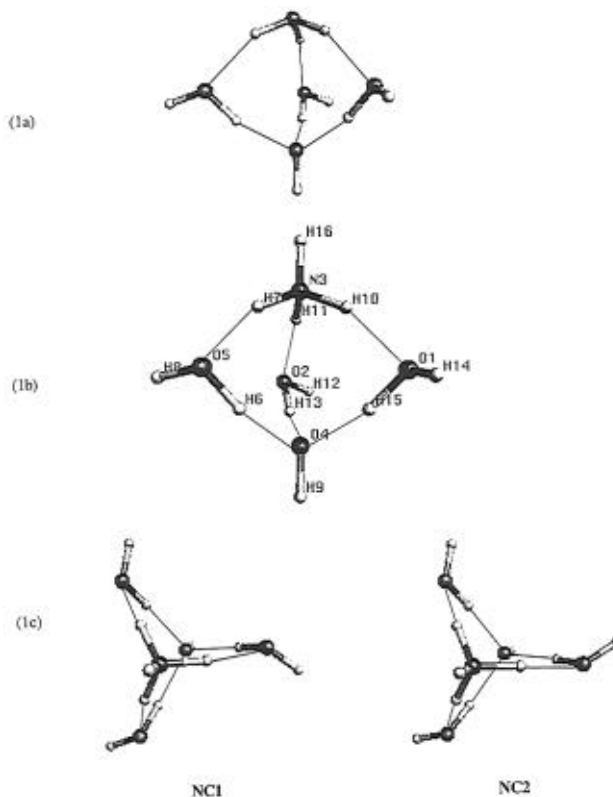


Figure 1. Frontal view of the $\text{H}_3\text{O}^+(\text{H}_2\text{O})_3\text{OH}^-$ and $\text{NH}_4^+(\text{H}_2\text{O})_3\text{OH}^-$ clusters (a and b, respectively, the later showing the atom-labeling convention). Perpendicular view of the NC1 and NC2 conformers of the $\text{NH}_4^+(\text{H}_2\text{O})_3\text{OH}^-$ cluster showing the different spatial arrangement.

a similar optimum geometry. The $\text{NH}_4^+(\text{H}_2\text{O})_3\text{OH}^-$ cluster thus formed has three water molecules between the two contraions. These waters are solvated against three of the hydrogens of the NH_4^+ ion via $\text{N}-\text{H}\cdots\text{O}$ hydrogen bonds in which the water acts as acceptor. At the same time, each solvated water makes a second $\text{O}-\text{H}\cdots\text{O}$ hydrogen bond with the oxygen atom of the OH^- ion acting as the acceptor.

Depending on the relative orientations of the three water molecules, one can obtain different conformers. We have selected two of them, hereafter identified as the NC1 and NC2 conformers (see Figure 1c). The geometries of these two conformers was then fully optimized at the HF, MP2, and BLYP levels using the usual minimization techniques. The three methods show the presence of a minimum of similar structure to that found for the $\text{H}_3\text{O}^+(\text{H}_2\text{O})_3\text{OH}^-$ cluster. These three minimum-energy structures were further characterized by computing their vibrational frequencies and all three structures were found to be a true minimum-energy structures. Therefore we can conclude that we have found local minima on the potential energy surfaces of the water-ammonia system.

To grasp the nature of these minimum energy structures, we decided to identify the fragments which form the cluster by analyzing the geometry of each cluster and its electronic distribution. We started by looking at the shortest inter or intramolecular distances among the atoms which constitute the cluster. Table 1 shows the values of the shortest intra (identified as $A_i - B_j$) and intermolecular (denoted as $A_i\cdots B_j$) contacts for the NC1 cluster (see Figure 1 for the atom labeling convention). The values for the NC2 cluster are so close that we decided do not include them. Also included in Table 1, for comparison, are the shortest intramolecular distances for the isolated neutral and ionic fragments which can be formed from the cluster.

TABLE 1: Shortest Intra- and Intermolecular Distances (A_i-B_j and $A_i\cdots B_j$, Respectively) within the Ionic NC1 Cluster and for the NH_4^+ , NH_3 , OH^- , and H_2O Fragments (See Figure 1 for the Atom Labeling of the NC1 Cluster. The Fragments are Numbered Subsequently)

parameter	method	compound				
		NC1	NH_4^+	NH_3	OH^-	H_2O
$\text{N}_3\text{-H}_{16}$	HF	1.002	1.012			
	MP2	1.013	1.023			
	BLYP	1.023	1.034			
$\text{N}_3\text{-H}_7^a$	HF	1.023	1.012	1.000		
	MP2	1.044	1.023	1.012		
	BLYP	1.068	1.034	1.022		
O_5H_8^b	HF	0.942				0.943
	MP2	0.963				0.963
	BLYP	0.974				0.974
$\text{O}_5\text{-H}_6^c$	HF	0.978				0.943
	MP2	1.021				0.963
	BLYP	1.045				0.974
$\text{O}_4\text{-H}_9$	HF	0.943			0.947	
	MP2	0.965			0.970	
	BLYP	0.973			0.980	
$\text{H}_7\cdots\text{O}_5^d$	HF	1.815				
	MP2	1.739				
	BLYP	1.716				
$\text{H}_{15}\cdots\text{O}_4^e$	HF	1.654				
	MP2	1.571				
	BLYP	1.559				

^a $\text{N}_3\text{-H}_7 = \text{N}_3\text{-H}_{10} = \text{N}_3\text{-H}_{11}$. ^b $\text{O}_5\text{-H}_8 = \text{O}_1\text{-H}_{14} = \text{O}_2\text{-H}_{12}$.
^c $\text{O}_5\text{-H}_6 = \text{O}_1\text{-H}_{15} = \text{O}_2\text{-H}_{13}$. ^d $\text{H}_7\cdots\text{O}_5 = \text{H}_{11}\cdots\text{O}_2 = \text{H}_{10}\cdots\text{O}_1$.
^e $\text{H}_{15}\cdots\text{O}_4 = \text{H}_{13}\cdots\text{O}_4 = \text{H}_6\cdots\text{O}_4$.

TABLE 2: Atomic Charges (in atomic units) for the Atoms of the Ionic NC1 Cluster and for the NH_4^+ , NH_3 , OH^- , and H_2O Fragments (See Figure 1 for the Atom Labeling of the NC1 Cluster. The Molecular Fragments are Numbered Consistently)

atom	method	compound				
		NC1	NH_4^+	NH_3	OH^-	H_2O
H_{16}	HF	0.36	0.43			
	MP2	0.35	0.42			
	BLYP	0.25	0.35			
N_3	HF	-0.82	-0.70	-0.88		
	MP2	-0.84	-0.69	-0.87		
	BLYP	-0.46	-0.38	-0.62		
H_7^a	HF	0.46	0.43	0.29		
	MP2	0.48	0.42	0.29		
	BLYP	0.30	0.35	0.21		
H_8^b	HF	0.37				0.37
	MP2	0.37				0.36
	BLYP	0.29				0.30
O_5^c	HF	-0.90				-0.74
	MP2	-0.93				-0.72
	BLYP	-0.68				-0.59
H_6^d	HF	0.52				0.37
	MP2	0.54				0.36
	BLYP	0.36				0.30
O_4	HF	-1.27			-1.24	
	MP2	-1.25			-1.24	
	BLYP	-0.92			-1.15	
H_9	HF	0.36			0.24	
	MP2	0.37			0.24	
	BLYP	0.29			0.15	

^a $\text{H}_7 = \text{H}_{10} = \text{H}_{11}$. ^b $\text{H}_8 = \text{H}_{12} = \text{H}_{14}$. ^c $\text{O}_5 = \text{O}_2 = \text{O}_1$. ^d $\text{H}_6 = \text{H}_{13} = \text{H}_{15}$.

The analysis of Table 1 results shows the presence of five molecular fragments with the following three chemical compositions: NH_4 , H_2O , and OH . One can use the electron distribution to determine the net charge on each fragment by looking at the net atomic charge on each atom as given by a Mulliken population analysis of the whole cluster wave function. The values for the NC1 and NC2 conformers are also nearly

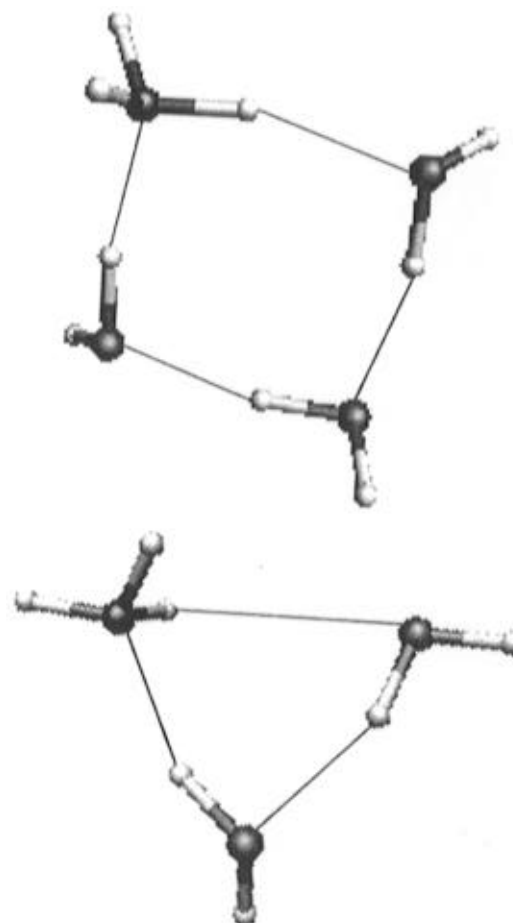


Figure 2. Tridimensional view of the fully optimized structures of the $\text{NH}_4^+(\text{H}_2\text{O})_2\text{-OH}^-$ and $\text{NH}_4^+(\text{H}_2\text{O})_1\text{-OH}^-$ clusters where one can see the absence of double-ionic forms.

identical, so we just included in Table 2 the results for the NC1 cluster. These numbers indicate that the HF and MP2 methods give similar atomic charges and that these charges are more ionic than these resulting from the BLYP computation: The net charge on the NH_4 and OH fragments is at the HF and MP2 levels close to +0.9 and -0.9, respectively, being the charge on the H_2O fragments close to zero. At the BLYP level, the charge on the H_2O fragments is also close to zero but that on the NH_4^+ and OH^- fragments is +0.6 and -0.6, respectively. The overall picture is that expected for the double-ionic $\text{NH}_4^+(\text{H}_2\text{O})_n\text{-OH}^-$ cluster. The cluster is more ionic at the HF and MP2 levels, while at the BLYP level our numbers indicate that there is a partial charge transfer from the negative fragment to the positive one. No studies have been carried out on this charge transfer either here or in the literature, but the fact that it is not also found at the MP2 level seems to indicate that is an artifact of the BLYP methodology.

The structure of these ionic clusters is very similar to that found for the other double-ionic clusters already computed (the $\text{H}_3\text{O}^+(\text{H}_2\text{O})_3\text{-OH}^-$ clusters and the double ionic $\text{H}_3\text{O}^+(\text{H}_2\text{O})_3\text{-A}^-$ clusters resulting from the ionic dissociation in water of an AH acid). In all cases the geometrical structure is one with the three water molecules located between the positive and negative contraions. We wanted to test if these double-ionic clusters are still stable when the number of water molecules is decreased to two or one. We performed this study on the NC1 cluster taking its optimum geometry, deleting one and two waters molecules and allowing the resulting $\text{NH}_4^+(\text{H}_2\text{O})_2\text{-OH}^-$ and $\text{NH}_4^+(\text{H}_2\text{O})_1\text{-OH}^-$ clusters to fully optimize. In both cases the geometry transforms spontaneously into the

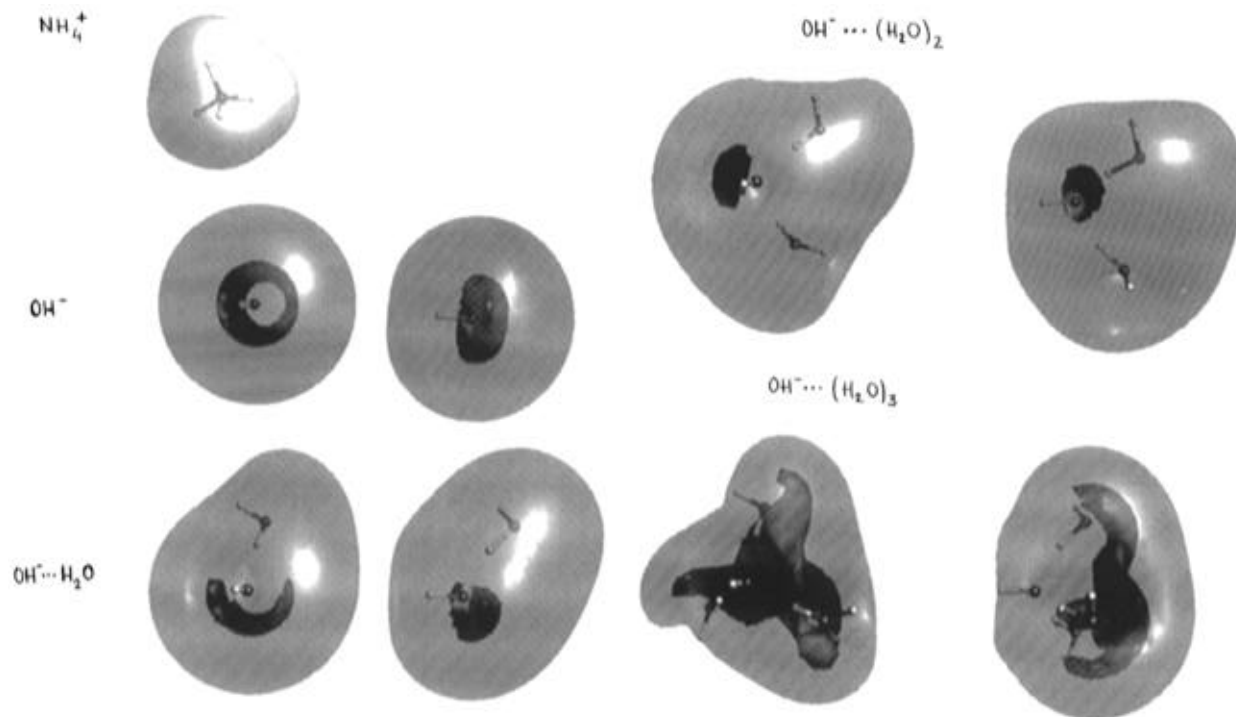


Figure 3. Molecular potential electrostatic maps (frontal and side views) for the NH_4^+ ion and the $\text{OH}^-\cdots(\text{H}_2\text{O})_n$, $n = 0, 1, 2, 3$ ions. In light is represented the positive (repulsive) region of +150 kcal/mol around the NH_4^+ ion. For the negative (attractive) potentials we are showing two regions: the darker color corresponds to the area around which the most stable potential is found (at values -237 kcal/mol for OH^- , -205 kcal/mol for $\text{OH}^-\cdots\text{H}_2\text{O}$, -175 kcal/mol for $\text{OH}^-\cdots(\text{H}_2\text{O})_2$, and -150 kcal/mol for $\text{OH}^-\cdots(\text{H}_2\text{O})_3$) and a lighter one at the values -113 kcal/mol for OH^- , -105 kcal/mol for $\text{OH}^-\cdots\text{H}_2\text{O}$, -90 kcal/mol for $\text{OH}^-\cdots(\text{H}_2\text{O})_2$, and -100 kcal/mol for $\text{OH}^-\cdots(\text{H}_2\text{O})_3$.

neutral structures shown in Figure 2 by transfer of a proton from the NH_4^+ to the OH^- ion. One can explain the absence of a minimum for the $\text{NH}_4^+(\text{H}_2\text{O})_2\text{OH}^-$ and $\text{NH}_4^+(\text{H}_2\text{O})_1\text{OH}^-$ doubly ionic clusters in simple terms by looking at the molecular electrostatic potentials of the NH_4^+ and the $\text{OH}^-\cdots(\text{H}_2\text{O})_n$, $n = 0, 1, 2, 3$ ions (see Figure 3). These maps show that when three molecules of water are present the OH^- potential is totally shielded and the most stable region of interaction of a positive charge with the $\text{OH}^-\cdots(\text{H}_2\text{O})_3$ fragment is on the water oxygens. When the number is decreased to two or just one, the OH^- becomes the location of the most attractive region for a positive charge. The NH_4^+ hydrogen feels this attraction and is transferred to the OH^- fragment. The transfer does not happen to the water given the stronger basicity of ammonia. These model and data nicely explains the absence of NH_4^+ and OH^- ions found in the experimental mono and dihydrate crystals, as was indicated above. The inclusion of more water molecules around the NC1 cluster as outer solvation sphere should further stabilize the ionic cluster through polarization and electrostatic effects. Therefore, the NC1 and NC2 clusters seem to be a promising structure for possible double-ionic clusters in larger water clusters or even in the bulk.

At this point, we decided to compare the predictions of the HF, MP2, and BLYP methods for the double ionic clusters. First of all, as mentioned above, the HF and MP2 atomic charges are pretty much the same and predict more ionic charge distributions than the BLYP method (see Table 2). This trend is also observed for the isolated ionic and neutral molecules (Table 2). We also notice from our data that the formation of a $\text{X-H}\cdots\text{Y}$ hydrogen bond within the cluster is reflected by an increase in the localized charge on the X and H atoms. In relation to the distances, we immediately notice that the similarity between the HF and MP2 results does not hold for the intra- and intermolecular distances (see Table 1). In this case, there is a systematic trend for the intramolecular distances,

in such a way that $r_{\text{intra}}(\text{HF}) < r_{\text{intra}}(\text{MP2}) < r_{\text{intra}}(\text{BLYP})$, while for the intermolecular distances the trend is just the opposite one, i.e., $r_{\text{inter}}(\text{HF}) > r_{\text{inter}}(\text{MP2}) > r_{\text{inter}}(\text{BLYP})$. The intramolecular distances for each cluster fragment are also similar to those computed with the same method for the corresponding isolated fragment.

We shifted our attention now to investigate the relative stability of the NC1 and NC2 clusters against neutral clusters of ammonia and water obtained from the double-ionic ones after geometrical arrangements. For such a purpose we computed the structure of several neutral ammonia-water clusters made up with one ammonia and four waters. We tested various reasonable geometrical arrangements and optimized their structures. The most interesting conformers are these shown in Figure 4. Two of them are ring structures (hereafter called NR1 and NR2) which differ in the number of $\text{N-H}\cdots\text{O}$ hydrogen bonds made by the ammonia molecule, one in the NC1 and two in the NC2 conformer. The third one is a neutral cluster whose structure is similar to that for the NC1 and NC2 double ionic clusters. Their structures were fully optimized at the HF, MP2, and BLYP levels. All of them were found to be true minimum-energy structures at the BLYP level. At the HF and MP2 levels, however, the NR2 minimum-energy structure computed using the BLYP functional spontaneously distorts into the much more stable NR3 structure. Therefore, only two minimum-energy structures (NR1 and NR3) are obtained.

The intra- and intermolecular distances for the NR1 and NR3 clusters are collected in Tables 3 and 4, and the corresponding atomic charges in Table 5. The values correspond to these for neutral fragments and confirm the non-ionicity within the cluster. The intramolecular distances for each fragment within the cluster are similar to those computed when isolated. The intra- and intermolecular distances follow the same trends already reported for the double ionic clusters, namely, $r_{\text{intra}}(\text{HF}) < r_{\text{intra}}(\text{MP2}) < r_{\text{intra}}(\text{BLYP})$ and $r_{\text{inter}}(\text{HF}) > r_{\text{inter}}(\text{MP2}) > r_{\text{inter}}(\text{BLYP})$. The

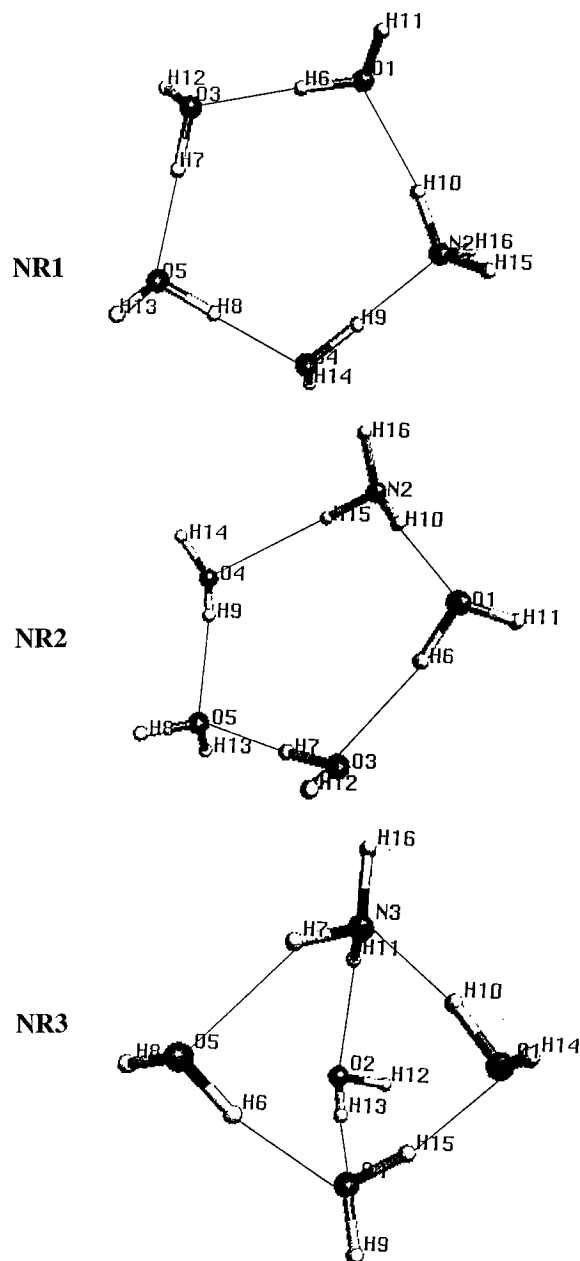


Figure 4. Tridimensional view of the neutral NR1, NR2, and NR3 conformers of the $\text{NH}_3\text{-(H}_2\text{O)}_4$ cluster showing their atom labeling convention.

structures do not show any particular feature except for the asymmetry between the $\text{N}_3\text{-O}_5\text{-O}_4$ and $\text{N}_3\text{-O}_2\text{-O}_4$ sides of the NR3 cluster.

The total energy associated with the optimum geometry of each neutral and double ionic cluster studied here and also for the isolated fragment is included in Table 6. With these values, we can investigate the relative stability of the double ionic clusters against the neutral ones and, on the other hand, the stability of these clusters against their dissociation into the neutral (NH_3 and H_2O) or ionic (NH_4^+ and OH^-) fragments (see also Table 6). Our results show that all the clusters, ionic or neutral, are stable against the two types of fragmentations. Furthermore, the MP2 and BLYP methods produce a similar interaction energy for all clusters, while the HF method provides interaction energies which are too small, in particular in the ionic clusters. Table 6 results also show that the dissociation into the ionic fragments is a lot less favorable than the dissociation into the neutral fragments.

TABLE 3: Shortest Intra- and Intermolecular Distances ($A_i\text{-}B_j$ and $A_i\cdots B_j$, Respectively) within the Neutral NR1 Cluster (See Figure 2 for the Atom Labeling)

parameter	method	distance (Å)
$\text{N}_2\text{-H}_{16}^a$	HF	1.002
	MP2	1.014
	BLYP	1.025
$\text{N}_2\text{-H}_{10}$	HF	1.006
	MP2	1.022
	BLYP	1.037
$\text{O}_1\text{-H}_{11}^b$	HF	0.943
	MP2	0.963
	BLYP	0.974
$\text{O}_1\text{-H}_6$	HF	0.953
	MP2	0.980
	BLYP	1.001
$\text{O}_3\text{-H}_7$	HF	0.954
	MP2	0.983
	BLYP	1.004
$\text{O}_5\text{-H}_8$	HF	0.955
	MP2	0.985
	BLYP	1.008
$\text{O}_4\text{-H}_9$	HF	0.960
	MP2	0.995
	BLYP	1.021
$\text{H}_{10}\cdots\text{O}_1$	HF	2.146
	MP2	1.994
	BLYP	1.978
$\text{H}_6\cdots\text{O}_3^c$	HF	1.926
	MP2	1.975
	BLYP	1.750
$\text{H}_8\cdots\text{O}_4$	HF	1.885
	MP2	1.744
	BLYP	1.695
$\text{H}_9\cdots\text{N}_2$	HF	1.972
	MP2	1.791
	BLYP	1.742

^a $\text{N}_2\text{-H}_{15} \cong \text{N}_2\text{-H}_{16}$. ^b $\text{O}_1\text{-H}_{11} \cong \text{O}_3\text{-H}_{12} \cong \text{O}_5\text{-H}_{13} \cong \text{O}_4\text{-H}_{14}$. ^c $\text{H}_6\cdots\text{O}_3 \cong \text{H}_7\cdots\text{O}_5$.

In relation with the relative stability of the ionic and neutral forms, Table 6 results show the following trend at the MP2 level: $\Delta E(\text{NR1}) < \Delta E(\text{NR3}) \ll \Delta E(\text{NC1}) < \Delta E(\text{NC2}) \ll \Delta E(\text{NR2})$. At this level, the ring-neutral form NR1 is about 2 kcal/mol more stable than the clustered form NR3, which is itself about 10 kcal/mol more stable than the NC1 and NC2 ionic conformers. The trend is very much the same for the HF and BLYP results. These results indicate that the formation of the double ionic clusters from the most stable neutral conformers is an endothermic process. However, the amount of energy required is not very large. In fact, at room temperature, it is in the range of the translational energy due to the thermal agitation. The energy differences computed here are also in good agreement with the experimentally determined ΔG value (6.48 kcal/mol, see above). If similar energy differences between the ionic and neutral are found in the bulk at room temperature, one can expect the formation of ionic NC1 and NC2 clusters from the neutral NR1 and NR3 clusters. When the zero-point energy corrections due to the vibrational motions are included (see numbers into parentheses in Table 6) all the clusters are still stable and the relative stability of one cluster against the others is more or less preserved because the difference between the zero-point correction for the clusters is nearly the same (about 10 kcal/mol). It is worthwhile to note here the similar zero-point energy obtained for the NC1 and NR1 when using the MP2 and BLYP methods. Except for small details, we can conclude that these two methods give a similar description of the structure and stability of the clusters studied here.

Our study shows the presence of stable double ionic structures (NC1 and NC2) which are local minimum on the potential

TABLE 4: Shortest Intra- and Intermolecular Distances (A_i-B_j and $A_i\cdots B_j$, Respectively) within the Neutral NR3 Cluster (See Figure 2 for the Atom Labeling of the NR3 Cluster)

parameter	method	distance (Å)
N_3-H_{16}	HF	1.001
	MP2	1.014
	BLYP	1.023
$N_3-H_7^a$	HF	1.003
	MP2	1.018
	BLYP	1.030
$O_5-H_8^b$	HF	0.947
	MP2	0.968
	BLYP	0.973
$O_5-H_6^c$	HF	0.946
	MP2	0.969
	BLYP	0.987
O_1-H_{10}	HF	0.961
	MP2	0.998
	BLYP	1.024
O_4-H_{15}	HF	0.956
	MP2	0.988
	BLYP	1.010
$H_7\cdots O_5$	HF	2.449
	MP2	2.295
	BLYP	2.168
$H_{11}\cdots O_2$	HF	2.546
	MP2	2.319
	BLYP	2.267
$H_{10}\cdots N_3$	HF	1.960
	MP2	1.773
	BLYP	1.735
$H_6\cdots O_4$	HF	2.345
	MP2	2.169
	BLYP	1.920
$H_{13}\cdots O_4$	HF	2.003
	MP2	1.885
	BLYP	1.915
$H_{15}\cdots O_1$	HF	1.879
	MP2	1.733
	BLYP	1.708

^a $N_3-H_7 \cong N_3-H_{11}$. ^b $O_5-H_8 \cong O_1-H_{14} \cong O_2-H_{12} \cong O_4-H_9$.
^c $O_5-H_6 \cong O_2-H_{13}$.

energy surface of a cluster of one ammonia and four water molecules. We have also found a similar neutral structure (NR3) which is more stable than the similar double ionic one. In fact, both structures are related by the transfer of H_{10} to O_1 and a posterior or simultaneous transfer of H_{15} to O_4 . This opens an interesting question: is this transfer process synchronous or asynchronous? Although our model system is very small, it is the simplest one we can use to represent the way the formation of the NH_4^+ and OH^- electrolytes in an ammonia-water solution, so the study of the synchronicity is important also for the ideas it can provide to understand such a process.

We have studied the synchronicity of the process $NR3 \rightarrow NC1$ using the BLYP functional and the TZ94P basis set, which we have seen above provides values for the geometry and the relative stability for both species similar to that given by the MP2 method. We did this study by computing the total energy as a function of the $H_{10}\cdots O_1$ and $H_{15}\cdots O_4$ distances, fully optimizing the geometry of all the other geometrical parameters in the complex. The resulting two-dimensional potential energy map, shown in Figure 5, shows the presence of two minima, corresponding to the NR3 (lower left corner) and NC1 (higher right corner) minima. Connecting these minima there is only one transition state. The transition state was fully characterized analytically: it is located at $d(H_{10}\cdots O_1) = 1.399$ Å and $d(H_{15}\cdots O_4) = 1.215$ Å and its total energy is at the BLYP level $-362.360\ 631$ atomic units, i.e., it lies 8.5 and 14.2 kcal/mol above the energy of the NC1 and NR3 conformers, respectively.

TABLE 5: Atomic Charges (in atomic units) for the Atoms of the Neutral NR1 and NR3 Clusters (See Figure 2 for the Atom Labeling of Both Clusters)

NR1			NR3		
atom	method	q_i	atom	method	q_i
H_{16}^a	HF	0.30	H_{16}	HF	0.30
	MP2	0.30		MP2	0.31
	BLYP	0.22		BLYP	0.22
N_2	HF	-1.00	N_3	HF	-1.00
	MP2	-1.00		MP2	-1.03
	BLYP	-0.71		BLYP	-0.72
H_{10}	HF	0.40	H_7^d	HF	0.35
	MP2	0.41		MP2	0.36
	BLYP	0.30		BLYP	0.27
O_1	HF	-0.83	H_8^e	HF	0.41
	MP2	-0.83		MP2	0.41
	BLYP	-0.67		BLYP	0.30
H_{11}^b	HF	0.37	O_5^f	HF	-0.79
	MP2	0.36		MP2	-0.80
	BLYP	0.29		BLYP	-0.64
H_6^c	HF	0.47	H_6^g	HF	0.41
	MP2	0.46		MP2	0.42
	BLYP	0.36		BLYP	0.34
O_4	HF	-0.85	O_4	HF	-0.88
	MP2	-0.84		MP2	-0.91
	BLYP	-0.67		BLYP	-0.69
H_9	HF	0.48	H_9	HF	0.39
	MP2	0.48		MP2	0.39
	BLYP	0.38		BLYP	0.31
			H_{15}	HF	0.47
				MP2	0.50
				BLYP	0.35
			O_1	HF	-0.84
				MP2	-0.88
				BLYP	-0.64
			H_{10}	HF	0.48
				MP2	0.51
				BLYP	0.34
			H_{14}	HF	0.37
				MP2	0.37
				BLYP	0.30

^a $H_{16} = H_{15}$. ^b $H_{11} = H_{12} = H_{13} = H_{14}$. ^c $H_6 = H_7 = H_8$. ^d $H_7 = H_{11}$.
^e $H_8 = H_{12}$. ^f $O_5 = O_2$. ^g $H_6 = H_{13}$.

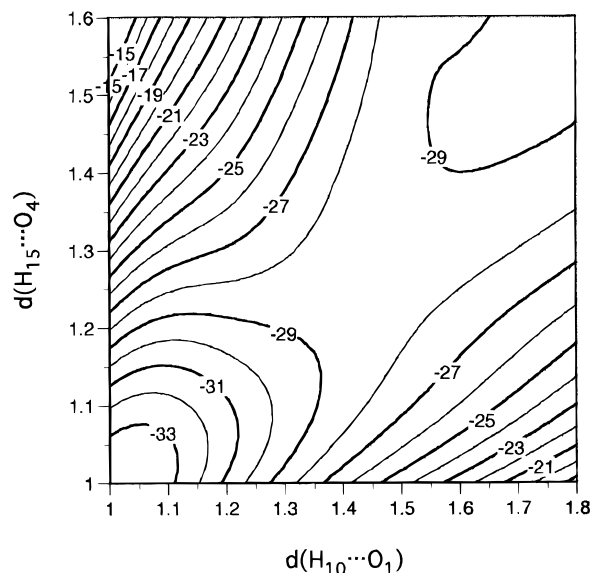


Figure 5. Potential energy map for the NR3 (lower left corner) to NC1 (upper right corner) transformation as a function the $H_{10}\cdots O_1$ and $H_{15}\cdots O_4$ distances. The energies (in kcal/mol) are interaction energies relative to the neutral fragments. The distances are given in angstroms.

This shows that the process of formation of the double ionic NC1 cluster from the neutral NR3 cluster is synchronous, i.e., the transfer of the H_{10} hydrogen to the O_1 atom with a positive

TABLE 6. Total Energy (First Row, in atomic units) and Intermolecular Interaction Energy Relative to the Neutral Fragments (Second Row, in kcal/mol), and Intermolecular Interaction Energy Relative to the Ionic Fragments (Third Row, in kcal/mol) for the Neutral and Ionic Clusters (Values in Parentheses Are the Corresponding Zero-Point Corrected Energies)

compound	method		
	HF	MP2	BLYP
H ₂ O	-76.031231	-76.233108	-76.442837
NH ₃	-56.200912	-56.392046	-56.556750
OH ⁻	-75.383956	-75.602111	-75.799452
NH ₄ ⁺	-56.545738	-56.734234	-56.892825
NC1	-360.334731 -5.58 (6.76) -195.37	-361.371452 -29.48 (-18.38) -210.71	-362.374197 -28.93 (-18.83) -221.77
NC2	-360.333963 -5.10 (6.97) -194.89	-361.370499 -28.88 -210.11	-362.372924 -28.13 (-18.11) -220.97
NR1	-360.375734 -31.31 (-21.16) -221.10	-361.390786 -41.61 (-30.89) -222.84	-362.391126 -39.55 (-29.38) -232.39
NR2	-360.351867 ^a -16.34 ^a -206.13 ^a	-361.358545 ^a -21.38 ^a -202.61 ^a	-362.357573 -28.50 (-18.53) -211.34
NR3	-360.371904 -28.91 (-18.75) -218.70	-361.387726 -39.69 -220.92	-362.383313 -34.65 (-24.12) -227.49

^a At the BLYP optimized geometry. It is not a minimum of this method.

charge induces the transfer of the H₁₅ hydrogen with also a positive charge to the O₄ atom. Although further studies with the inclusion of more water molecules are needed before allowing to make proper extrapolations to the bulk, the results shown in Figure 5 give a first glimpse on how process 1 can take place in the bulk.

Concluding Remarks

Using the Hartree–Fock, second-order Moller–Plesset methods, and the Becke–Lee–Yang–Parr density functional, we have shown the existence of a minimum energy in the potential energy surface of four water and one ammonium molecules for the NH₄⁺⋯(H₂O)₃⋯OH⁻ cluster. This cluster (either NC1 or NC2) is the result of one proton transfer from one of the water molecules to the ammonia molecule. Its structure is similar to that for the other BH⁺⋯(H₂O)₃⋯OH⁻ clusters, already computed with three water molecules between the NH₄⁺ and OH⁻ ions. With less than three water molecules it seems that no double ionic cluster is formed. Although the ionic cluster is stable against its dissociation into their constituent neutral and

ionic fragments its energy lies about 5 kcal/mol above that for its neutral equivalent (NR3). The process of formation of NC1 from NR3 is shown to be a synchronic one in which two protons are simultaneously transferred. The BLYP method gives a description of the structure and stability of these clusters similar to the MP2 method.

Acknowledgment. The authors thank the management of Cray Research, Inc., for enabling and supporting this work and CESCO, the “Centre de Supercomputació de Catalunya” (Catalunya, Spain), for a grant in computer time. This work was also supported by the DGICYT and CIRIT under Projects PB-92-0655-C02-02 and GRQ94-1077. M.P. thanks the Spanish Science and Education Department for his doctoral grant.

References and Notes

- (1) See, for instance: Bell, R. P. *The Proton in Chemistry*, 2nd ed.; Chapman and Hall: London, 1973.
- (2) Perrin, D. B. *Ionization Constants of Inorganic Acids and Bases in Aqueous Solution*, 2nd ed.; Pergamon: Oxford, 1982.
- (3) Kebarle, P. *Annu. Rev. Phys. Chem.* **1977**, *28*, 445.
- (4) Waldron R. D.; Hornig, D. F. *J. Am. Chem. Soc.* **1953**, *75*, 6079.
- (5) Moruzzi J. L.; Phelps, A. V. *J. Chem. Phys.* **1966**, *45*, 4617. De Paz, M.; Guidini Giardini, A.; Friedman, L. *J. Chem. Phys.* **1970**, *52*, 687. Meot-Ner, M.; Speller, C. V. *J. Phys. Chem.* **1986**, *90*, 6616. Deakyne, C. A. *J. Phys. Chem.* **1986**, *90*, 6625.
- (6) Newton, M. D.; Ehrenson, S. *J. Am. Chem. Soc.* **1971**, *93*, 4971. Sapsee, A. M.; Osorio, L.; Snyder, G. *Int. J. Quantum Chem.* **1984**, *26*, 223. Pople, J. A.; Curtiss, L. A. *J. Phys. Chem.* **1987**, *91*, 155. Del Bene, J. E. *J. Phys. Chem.* **1988**, *92*, 2874. Kassab, E.; Evleth, E. M.; Hamou-Tahra, Z. D. *J. Am. Chem. Soc.* **1990**, *112*, 103.
- (7) Lee, C.; Sosa, C.; Novoa, J. J. *J. Chem. Phys.* **1995**, *103*, 4360.
- (8) Lee, C.; Sosa, C.; Planas, M.; Novoa, J. J. *J. Chem. Phys.*, submitted.
- (9) GAUSSIAN-92, Revision D2; Frisch, M. J.; Trucks, G. W.; Head-Gordon, M.; Gill, P. M. W.; Wong, M. W.; Foresman, J. B.; Johnson, B. G.; Schlegel, H. B.; Robb, M. A.; Replogle, E. S.; Gomperts, R.; Andres, J. L.; Raghavachari, K.; Binkley, J. S.; Gonzalez, C.; Martin, R. L.; Fox, D. J.; Defrees, D. J.; Baker, J.; Stewart, J. J. P.; Pople, J. A. Gaussian, Inc.: Pittsburgh, PA, 1992.
- (10) Becke, A. D. *Phys. Rev. A*, **1988**, *38*, 3098. Becke, A. D. *J. Chem. Phys.* **1992**, *96*, 2155.
- (11) Lee, C.; Yang, W.; Parr, R. G. *Phys. Rev. B* **1988**, *37*, 785.
- (12) DGAUSS is a software product available from Fray Research Inc. a part of the UniChem software package. For details of the Dgauss methodology see: Andzelm, J.; Wimmer, E. *J. Chem. Phys.* **1992**, *96*, 1280.
- (13) Lee, C.; Chen, H.; Fitzgerald, G. *J. Chem. Phys.* **1995**, *102*, 1266. Lee, C.; Chen, H.; Fitzgerald, G. *J. Chem. Phys.* **1994**, *101*, 4472.
- (14) Sim, F.; St-Amant, A.; Papai, I.; Salahub, D. R. *J. Am. Chem. Soc.* **1992**, *114*, 4391.
- (15) Laasonen, K.; Parrinello, M.; Car, R.; Lee, C.; Vanderbilt, D. *Chem. Phys. Lett.* **1993**, *207*, 208.
- (16) Kim, K.; Jordan, K. D. *J. Phys. Chem.* **1994**, *98*, 10089.
- (17) Xantheas, S. S. *J. Chem. Phys.* **1995**, *102*, 4505.
- (18) Novoa, J. J.; Sosa, C. *J. Phys. Chem.* **1995**, in press.
- (19) Lee, C.; Stahlberg, E.; Fitzgerald, G. *J. Phys. Chem.*, submitted.

JP953360V